View Article Online
View Journal

Photochemical & Photobiological Sciences

An international journal

Accepted Manuscript

This article can be cited before page numbers have been issued, to do this please use: K. A. D. F. Castro, L. D. Costa, S. Guieu, J. Biazzoto, M. D. G. P. M. S. Neves, M. A. Faustino, R. Santana da Silva and A. Tomé, *Photochem. Photobiol. Sci.*, 2020, DOI: 10.1039/D0PP00114G.

ROYAL SOCIETY OF CHEMISTRY

rsc.li/pps

View Article Online
DOI: 10.1039/D0PP00114G

ARTICLE

Photodynamic treatment of melanoma cells using aza-dipyrromethenes as photosensitizers

Received 00th January 20xx,
Accepted 00th January 20xx

DOI: 10.1039/x0xx00000x

Kelly A. D. F. Castro,[a†*] Letícia D. Costa,[b†] Samuel Guieu,[b,c] Juliana C. Biazzotto,[a] Maria da Graça P. M. S. Neves,[b] M. Amparo F. Faustino,[b*] Roberto S. da Silva,[a*] and Augusto C. Tomé[b*]

This work provides the first study about the use of four aza-dipyrromethenes (ADPMs) as photosensitizers for cancer PDT. The synthesis and characterization of the ADPMs and their photodynamic action against B16F10 melanoma cells was assessed. The ADPM **2** is the best singlet oxygen generator and the most phototoxic (at 2.5 μM) towards B16F10 cells.

Introduction

Aza-dipyrromethenes (ADPM) are a class of deep blue organic chromophores first synthesized in 1943.[1,2] Despite endowed with fascinating features, the ADPM derivatives were underestimated during decades[3] but, thanks to the excellent work developed by O'Shea and co-workers, the interest for this family of chromophores was rekindled.[3,4] Noteworthy, this research group reported, in 2012, a mechanistic analysis providing a deep understanding about the intermediates involved in the synthesis of these derivatives.[5] Although the retrosynthetic approach based on the mechanism has led to the development of other methodologies,[6,7] these compounds are still predominately synthesized from diaryl-nitro ketone precursors, although using the milder reaction conditions proposed and optimized by O'Shea's group in 2004.[3]

The great interest of these compounds lies in the intense and broad absorption they exhibit, as well as on their excellent stability.[8] Beyond that, the possibility of quickly fine-tune their photophysical properties through the introduction of additional functional groups or even through small post-modifications reactions, such as the formation of boron chelates (BF_2 or $B(OR)_2$)[9-11] or the coordination with metal ions (*e.g.,* Zn(II), Au (III), Hg (II), Re(I), Pd(II), Pt(II)),[8,12-20] has boosted their exploitation in a wide range of applications, namely in biological and material sciences. Among the applications with major relevance, we can highlight the use of these compounds as photosensitizers (PS) for photodynamic therapy (PDT), as fluorescent probes for *in vitro* or *in vivo* imaging, as chemosensors, or even as light harvesters in organic photovoltaic devices.[12,21-23] However, the potential of the ADPM backbone by its own is still neglected, because it is regarded as a mere precursor to obtain boron difluoride chelates (aza-BODIPYs). As far as we known, nothing has yet been described about the potential applications of these ligands alone. In this communication, we report a preliminary evaluation concerning the ability of these compounds to act as PS for the photodynamic therapy (PDT) of melanoma cancer cells. The choice of this cell model was not aleatory. In fact, melanoma is one of the most aggressive and deadliest form of skin cancer, and its incidence worldwide is increasing fast.[24-26] Moreover, the heterogeneity and the remarkable predisposition of these tumours for metastatic spreading are responsible for their poor response to conventional therapies.[26-29] Therefore, there is an urgent need to develop alternative or combined strategies able to overcome this resistance and lack of response. In the last few years, the PDT emerged as a promising approach for the treatment of skin cancers, mainly due to its minimally invasive nature, low side effects and excellent aesthetic outcome.[27,28] Indeed, as evidenced by the significant increase in number of clinical trials registered and authorised, PDT is now widely used in European countries, and therefore all attempts to find new photosensitizers or improve this therapeutic approach must be considered.[30] In this work, we synthesized four ADPMs bearing different substituent groups on the phenyl rings (-H, -OMe or $-NMe_2$), in order to determine the impact of these substituents either on the photophysical properties and on their biological activity towards the resistant melanoma cell line B16F10. As far we known, this is the first study to evaluate the use ADMs as photosensitizers for PDT.

Experimental

Synthesis and photophysical properties

[a.] *Department of Physics and Chemistry, Faculty of Pharmaceutical Sciences of Ribeirão Preto, University of São Paulo, SP, Brazil.*
[b.] *LAQV-REQUIMTE, Department of Chemistry, University of Aveiro, Portugal.*
[c.] *CICECO – Aveiro Institute of Materials, Department of Chemistry, University of Aveiro, Portugal.*
†These two authors contributed equally to this work.
*Corresponding authors
Electronic Supplementary Information (ESI) available: [details of any supplementary information available should be included here]. See DOI: 10.1039/x0xx00000x

View Article Online
DOI: 10.1039/D0PP00114G

Unless otherwise stated, all chemicals were used as supplied. Analogously, all solvents were used as received or purified by distillation prior to use. ADPM **1–4** were synthesized through the condensation of the adequate 1,3-diaryl-4-nitrobutan-1-ones, following reported procedures (Scheme 1).[3] After purification by column and thin-layer chromatography, the structures of all compounds were confirmed by nuclear magnetic resonance (NMR) and mass spectrometry (MS).

ADPM 1 (Yield: 44%), ^{1}H-NMR (300 MHz, $CDCl_3$): δ 8.08–8.04 (m, 4H), 7.98–7.94 (m, 4H,), 7.57–7.34 (m, 12H), 7.21 (s, 2H). MALDI-MS: *m/z* 450.373 for $[M+H]^+$. UV-Vis (DMF) λ_{max}, (log ε): 306 (4.28) and 604 (4.32). **ADPM 2** (Yield: 41%) ^{1}H-NMR (300 MHz, $CDCl_3$): δ 8.05–8.00 (m, 4H), 7.95–7.92 (m, 4H), 7.55–7.43 (m, 6H), 7.10 (s, 2H), 6.99–6.94 (m, 4H), 3.89 (s, 6H). MALDI-MS: *m/z* 510.254 for $[M+H]^+$. UV-Vis (DMF) λ_{max}, (log ε): 302 (4.36) and 615 (4.43).; **ADPM 3** (Yield: 45%) ^{1}H-NMR (300 MHz, $CDCl_3$): δ 8.05–8.00 (m, 4H), 7.90–7.85 (m, 4H), 7.06–7.02 (m, 6H), 6.98–6.93 (m, 4H), 3.91 (s, 6H), 3.88 (s, 6H). MALDI-MS: *m/z* 570.244 for $[M+H]^+$. UV-Vis (DMF) λ_{max}, (log ε): 304 (3.78) and 632 (3.86); **ADPM 4** (Yield: 20%) ^{1}H-NMR (300 MHz, $CDCl_3$): 8.05 (d, *J* = 8.8 Hz, 4H), 7.89 (d, *J* = 8.8 Hz, 4H), 7.04 (d, *J* = 8.8 Hz, 4H), 6.99 (s, 2H), 6.79 (d, *J* = 8.8 Hz, 4H), 3.91 (s, 6H), 3.04 (s, 12H). MALDI-MS: *m/z* 596.283 for $[M+H]^+$. UV-Vis (DMF) λ_{max}, (log ε): 323 (3.93) and 656 (3.85). Additional experimental details are provided in the Supporting Information (SI). Electronic spectra (UV-Vis) were obtained on an Agilent 8453 spectrophotometer, in the 200–800 nm wavelength range in different solvents (chloroform, dichloromethane, DMF, DMSO or ethanol). The fluorescence emission spectra were recorded under normal atmospheric conditions on a computer controlled F4500 – Hitachi spectrofluorimeter, using 1 × 1 cm quartz optical cells and solvents of various polarities (dichloromethane, DMF, DMSO or ethanol). The widths of both excitation and emission slits were set at 5.0 nm and the optical density of all the samples was 0.05. The singlet oxygen ($^1O_2$) production was determined by an indirect method that uses 1,3-diphenylisobenzofuran (DPiBF) as $^1O_2$ scavenger.[31] Briefly, DMF solutions containing 0.5 μM of each ADPM and 50 μM of DPiBF were irradiated with a LED array with an emission peak centered at 640 nm. The breakdown of DPiBF, indicative of singlet oxygen production, was determined through the follow-up of the absorbance decrease at 415 nm, during 6 min and at irradiation intervals of 1 min. 5,10,15,20-tetraphenylporphyrin (TPP), a well-known singlet oxygen producer, was used as reference (ϕ_Δ = 0.64 in DMF).[32]

Biological studies

Cell Culture

All cytotoxicity assays were performed against the highly metastatic murine melanoma cell line B16F10, purchased from the American Type Culture Collection (ATCC no. CRL-6475). B16F10 cells were grown as monolayers in Roswell Park Memorial Institute (RPMI) 1640 medium supplemented with 10% (v/v) heat inactivated fetal bovine serum, 100 IU mL^{-1} penicillin G, 100 mg mL^{-1} streptomycin, and 1 μg mL^{-1} amphotericin, in a humidified atmosphere of 95% air and 5% CO_2, at 37 °C.

Dark Cytotoxicity and Photodynamic Treatment

For the cytotoxicity studies, stock solutions of each ADPM with appropriate concentrations were prepared in DMSO and subsequently diluted in RPMI in order to ensure that the final concentration of DMSO in the culture medium was always 1% (v/v). To evaluate the dark cytotoxicity and the phototoxicity, cultures of B16F10 cells were prepared in 96-well plates, at a seeding density of 2 × 10^4 cells/well. The cells were then incubated for 24 h at 37 °C, in a CO_2 incubator. Then, ADPMs **1–4** were added to the culture medium in each corresponding wall, and their final concentrations ranged from 2.5 to 80 μM. The 96-well plates were incubated for 4 h at 37 °C, in a CO_2 incubator, in the dark, before irradiation. After the dark incubation, the cells were rinsed with PBS and fresh RPMI medium without phenol red was added. Lastly, the cell cultures were irradiated with a homemade set of 96 light-emitting diodes with emission band between 600 to 650 nm at an irradiance of 13.9 mW/cm^2, wherein the total light dose was 5 J/cm^2 or 10 J/cm^2. After irradiation, the cells were incubated for further 20 h in the dark and the cell viability was then determined by the MTT assay.[33] For the dark cytotoxicity evaluation, the cells were treated and processed under the same conditions described for PDT studies, but were kept always in the dark. Light controls (cells without ADPM but irradiated under the same light conditions) were performed in parallel. At least three independent assays were performed in triplicate for each condition. The cellular uptake of ADPM **1–4** (20 μM) after 4 h was analysed by fluorescence microscopy using a Nikon Eclipse Ti Microscope model TI-FL. The cells were marked with specific organelles staining probes (Rhodamine 123 for mitochondrial membranes and Hoechst 33342 for the nuclei).

Statistical Analysis

All statistical analyses were performed using GraphPad Prism 7. The results were reported as the mean ± standard deviation. The significance of dark or photodynamic treatment of each compound on the cell viability was assessed by an unvaried analysis of variance ANOVA. Multiple comparisons were performed with the Bonferroni's post hoc test. P<0.05 was considered significant.

LogP in silico calculations

The miLogP was calculated using Molinspiration WebME Editor 3.81. The parameters for drug-likeness were evaluated according to the Lipinski's 'rule-of-five', using the Molinspiration WebME Editor.[34] The parameters determined are summarized in Table S2 in the SI.

Results and Discussion

Synthesis and photophysical properties

View Article Online
DOI: 10.1039/D0PP00114G

The ADPMs **1–4** selected for this study were obtained according to the synthetic route summarized in Scheme 1. A base-catalysed aldol condensation involving the adequate aldehydes and acetophenones afforded the required chalcones.[1,2] The subsequent Michael addition of nitromethane to these α,β-unsaturated ketones yielded the 1,3-diaryl-4-nitro-butan-1-ones.[35] The desired ADPMs were obtained from the reaction of the nitroketones with an excess of ammonium acetate (NH_4OAc) in refluxing ethanol.[3] ADPMs **1–4** were obtained in moderate yields (20–45%) after purification by column or thin-layer chromatography. The low yield of ADPM **4** when compared with the other ADPM derivatives can be ascribed to the dimethylamine groups present in its constitution, and which hinder the purification process. Actually, these basic dimethylamine groups strongly interact with the acidic silanol groups on the silica, so that part of the product may have been lost during the purification process. The identity of all compounds and intermediates was confirmed by NMR and MS (Figs. S1–S8 in SI).

The photophysical characterization of all ADPMs was performed in various solvents (CH_2Cl_2, $CHCl_3$, DMF, DMSO and ethanol). All ADPMs exhibit a strong and broad absorption band between 500 to 800 nm, assigned to π–π* transitions (Figure 1).

ADPMs are solvent-sensitive molecules, and the absorption maxima are dependent on the solvent polarity (Table S1 in the SI). The fluorescence emission profile of each ADPM upon excitation at *ca.* 600 nm was also investigated (Figure S9 and Table S1 in the SI). As expected, these compounds are weakly emissive when compared with the TPP used as fluorescence reference (Figure S10), which made the accurate determination of the fluorescence quantum yields (ϕ_F) difficult. Actually, unlike the aza-BODIPYs that emit in the red-NIR region with a high quantum yield (ϕ_F), the ADPM ligands are non-emissive or weakly emissive at room temperature.[8] This behaviour is usually ascribed to the lack of structural rigidity, which is pointed out as the main reason for the nonradiative deactivation from the excited state.[8] Indeed, both the rotation of the aryl rings and the tautomerism that can occur via intramolecular proton transfer between the two adjacent pyrrole units can contribute to the non-emissive profile of these compounds.[8,36] It is widely known that the absorption and emission maxima is influenced by the substitution pattern. As expected, the introduction of

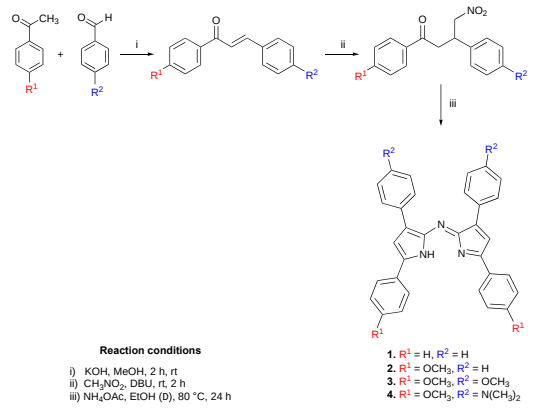

Scheme 1. Synthetic route to ADPMs **1–4**.

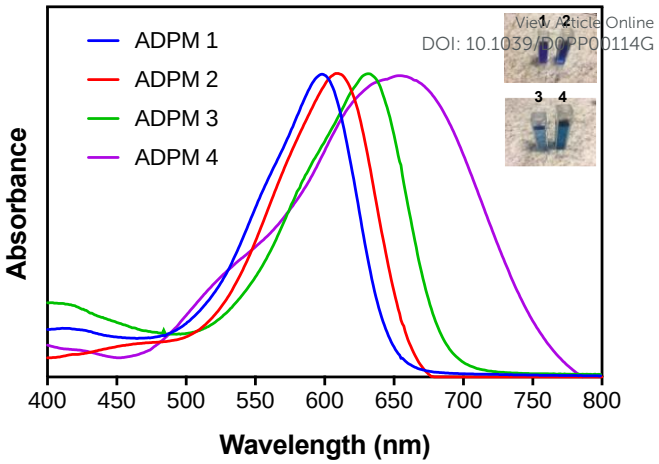

Figure 1. Normalized UV-Vis spectra and visual appearance of ADPMs in DMF solution.

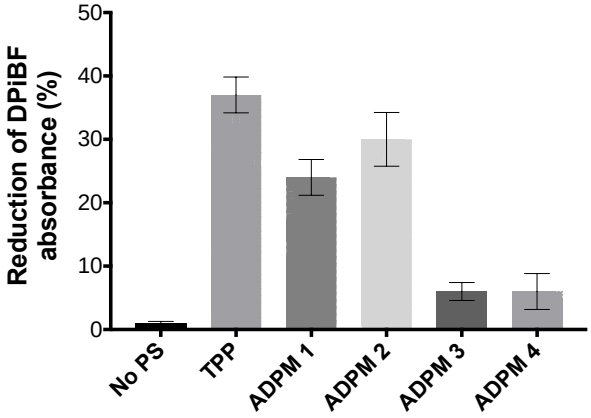

Figure 2. Reduction of the absorbance of DPiBF after irradiation with LEDs array (λ = 640 nm) at an irradiance of 13.9 mW/cm² in the presence of ADPMs at a concentration of 0.5 μM in DMF.

electron-donating groups (OMe or NMe_2) induced a bathochromic displacement of both the absorption and emission maxima.[37] The solvent used to acquire the absorption and the emission spectra is also relevant as, with the exception of ADPM **1**, all ADPMs exhibit a solvatochromic behaviour.

The singlet oxygen ($^1O_2$) generation was determined through the photooxidation of 1,3-diphenylisobenzofuran (DPiBF) by the singlet oxygen produced in consequence of ADPM's photosensitization.

For these experiments, the concentration of each ADPM was 0.5 μM and that of DPiBF was 100 times higher. The results obtained are gathered in Figure 2. Looking at these results, it must be stressed that the production of $^1O_2$ by the ADPM **2** is only slightly lower than that observed for TPP, which is considered a good $^1O_2$ producer (Φ_Δ = 0.64 in DMF).[32] In turn, the ability of ADPMs **3** and **4** to generate $^1O_2$ is relatively poor in DMF. Indeed, the negligible generation of $^1O_2$ by compounds **3** and **4** can be justified by the presence of the electron-donating R^2 groups. In fact, it is already documented in the literature that the introduction of electron-donating groups (OMe or -NMe_2) can hamper the production of singlet oxygen.[38,39] In addition, the trend of these compounds to aggregate in solution can also be responsible for this result. Beyond the ability to produce

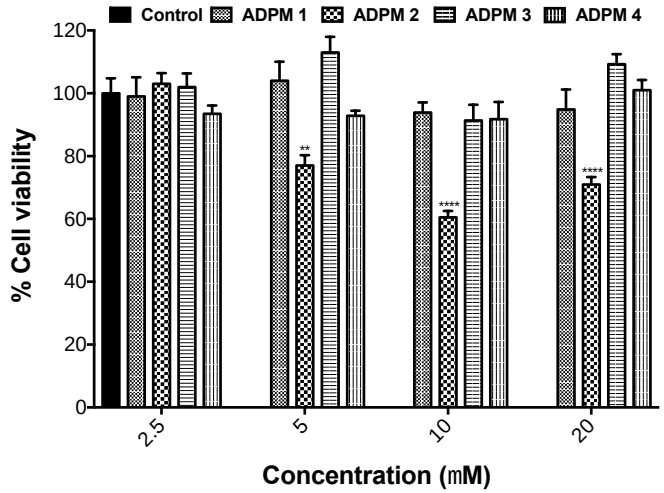

Figure 3. The cytotoxic effect of ADPM **1–4** against the B16F10 cell line under dark conditions was determined by the MTT assay. All experimental conditions were performed in three independent experiments and in triplicate and expressed as the mean ± standard deviation. Statistical significance against non-treated cells: **: p value < 0.01; ***p < 0.001 and ****p < 0.0001.

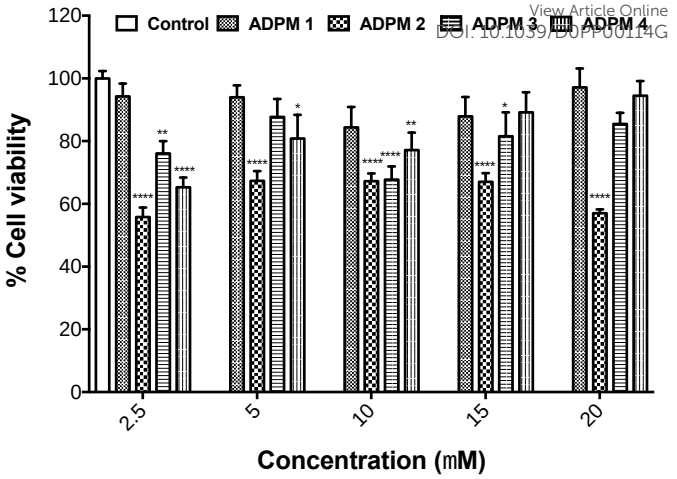

Figure 4. The photodynamic activity of ADPMs 1–4 against the B16F10 cell line was determined by the MTT assay. Cell cultures were irradiated with a red light (λ = 640 nm) LEDs array, at an irradiance of 13.9 mW/cm^2, and a total light dose of 10 J/cm^2. All experimental conditions were performed in three independent experiments and in triplicate and expressed as the mean ± standard deviation. Statistical significance against non-treated cells: *: p value < 0.05; **p < 0.01 and ****p < 0.0001.

reactive oxygen species (ROS), namely singlet oxygen, the photostability and solubility of these compounds in the biological environment are important factors since can determine the efficiency of the photodynamic treatment. The drug-likeness properties of these compounds were quantified by *in silico* calculations (Table S2). Noteworthy, all ADPMs are poorly water-soluble as all of them exhibited octanol–water partition coefficients (milog *P*) greater than 5. In fact, it must be stressed that hydrophobic compounds with a strong tendency to aggregate in the biological media usually have a diminished activity as result of its lower bioavailability in the target tissue.[40-42] Apart from the *in silico* calculations, the aggregation behaviour of these compounds was evaluated in RPMI medium containing 1% of DMSO by monitoring the UV- Vis profile (Figure S11 for ADPM **2**). The absence of a linear relationship clearly demonstrates the formation of aggregates. The photostability of all ADPMs was also evaluated by UV-Vis spectroscopy, by irradiation of a solution of the ADPM in DMSO/PBS, under the same light conditions of the PDT experiments. All ADPM are photostable at concentrations for which the aggregation is minimized (data not shown).

Biological studies

The broad absorption of ADPM derivatives within the so called "therapeutic window", and their high extinction coefficients led us to exploit the potential of these compounds as photosensitizing agents for PDT. In the first assays concerning the biological activity of these ADPMs against the resistant melanoma cell line B16F10, the cellular toxicity in the dark and after irradiation was evaluated at concentrations of 10, 20, 40 and 80 μM (Figures S12 and S13 in the SI). The results obtained seems to indicate that the cell viability in the presence of ADPM derivatives was not significantly affected neither by the increase in the PS concentration nor by the light irradiation. Indeed, these results can be explained by the hydrophobic character of these compounds, corroborated by *in-silico* calculations (Table S2 in the SI), and the occurrence of aggregation phenomena for concentrations higher than 20 μM. Nevertheless, considering the results of the cytotoxic effect and the photodynamic activity, it is evident that the ADPM **2** is an effective PS to kill the resistant melanoma cells herein studied.

Taking the conclusions above mentioned into account, we decided to evaluate the biological behaviour of these compounds at lowest concentrations (Figures 3 and 4). In turn, it must be stressed that the decrease in the concentration of ADPM administered was offset by increasing the light dose from 5.0 to 10 J/cm^2. As we had suspected, the reduction of the dose of ADPM administered lead to a better photodynamic performance. Notwithstanding the significant decrease in the concentration of ADPM administered to the cells, the formation of aggregates was still evident for the highest concentrations. Since the aggregation of a given PS is intrinsically related with the loss or diminished photodynamic activity, it is not so surprising that the best photodynamic results were achieved with the lowest tested concentration (2.5 μM). In practice, the photodynamic treatment with 2.5 μM of each ADPM (**1–4**) and a total light dose of 10 J/cm^2 lead to a decrease of 6, 44, 24 and 35% in cell viability, respectively, while at the concentration of 20 μM (8 times higher) the cell viability increase and was over 85% for ADPMs **1**, **3** and **4**. For ADPM **2**, the cell viability remained at 43±1.2%. However, it is worth to mention that a similar cell viability reduction was observed under dark conditions for ADPM **2** at concentrations of 10 and 20 μM (≈ 40%), which means that, at these concentrations, this ADPM **2** exhibits cytotoxicity. Nevertheless, none of the tested compounds, including the ADPM **2**, are cytotoxic at a concentration of 2.5 μM, which demonstrate clearly the potential of ADPM **2** as PS against B16F10 melanoma cell line, at this concentration.

The light dose effect (5.0 or 10 J/cm^2) was also evaluated by comparing the cell viability after the photodynamic treatment with 20 μM of each ADPM. Overall, the total light dose had influence on the cell viability only for ADPMs **2** and **3**. In fact, while the activity of ADPM **2** increased from 25 to 43%, the

View Article Online
DOI: 10.1039/D0PP00114G

ADPM **3** passed from a state of non-activity to a modest decrease of the cell viability in *ca.* 15%.

O'Shea and co-workers described the synthesis of some aza-BODIPYs, including the BF_2-chelates of the ADPMs **1** and **2**. Beyond the synthesis and photophysical characterization of the synthesized compounds, they also evaluated the biological activity of these compounds against MRC5-SV40 transformed fibroblasts and HeLa cells.[3] Interestingly, while in our study the ADPM **2** exhibited the highest phototoxicity, in O'Shea's work the BF_2-chelate of **1** exhibited the best results in both cell lines. Noteworthy, it must be stressed that they have used Cremophor EL, a non-ionic surfactant commonly used as delivery vehicle of hydrophobic drugs, thereby avoiding the loss of activity that we had as a result of aggregation phenomena. Moreover, they also used a higher total light dose (16 J/cm^2) than the maximum light dose that we used in this study (10 J/cm^2). Recently, Silva and co-workers[33] studied the antitumoral activity of a BODIPY containing a ruthenium(II) complex bearing aminopropyl lactose units in the ligands, against the B16F10 cell line. Briefly, the authors reported a dose-dependent activity, that resulted in a decrease in the cell viability by 50% for a concentration of 100 μM, but of less than 5% for a concentration of 2.0 μM. Therefore, if we compare our results with those reported by Silva, it becomes clear that, for lower concentrations, our compounds exhibited a much higher activity. In addition, the cytotoxicity of the ADPMs studied here towards B16F10 cells is comparable to that induced by other BODIPYs.[43]

Although the compounds are weakly emissive, we tried to monitor the cellular uptake of these ADPMs by B16F10 cells through fluorescence microscopy. Briefly, ADPM **1–4** (20 μM) were incubated in the same conditions used for the cytotoxicity assays, for periods ranging from 1 to 4 h. Fortunately, the images acquired for ADPM **3** allowed us to conclude that the cellular uptake was time dependent (see Figure S14). Although no fluorescence emission was detected for compounds **1** and **2**, we believe that a similar internalization also occurred. Indeed, although no fluorescence emission was detected for ADPM **2**, the PDT assays shows phototoxicity, which supports their internalization by B16F10 cells. The subcellular localization of these ADPMs was also evaluated by fluorescence microscopy. Indeed, the determination of the cellular localization of a given PS within the target cells is of paramount importance, because this is what determines the site of primary photodamages and the type of cellular response to the therapy.[44]

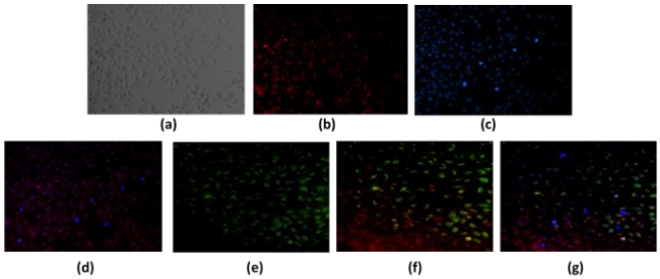

Figure 5. Intracellular localization of ADPM **3**. The B16F10 cells were treated with 20 μM of ADPM **3** for 4 h and subsequently loaded with Hoechst nucleus probe, Rhodamine 123 mitochondrial probe and then subjected to imaging microscopy. (a) bright field images, (b) ADPM **3** internalized; (c) cells marked with Hoechst, (d) Merged of b and c; (e) cells marked with Rhodamine 123; (f) Merged of b and e; (g) Merged of b, c and e.

The intracellular localization of ADPM **3** is depicted in Figure 5. In the same way as for BODIPY-like compounds, this ADPM was preferably located within lipophilic organelles.[45] In practice, the images showed that the ADPM **3** is uniformly distributed inside the cells (Figure 5b), but is not co-located with the nucleus (Figure 5d). The co-localization of ADPM **3** with rhodamine (Figure 5f) suggests that this compound was localized in the mitochondria. Cosa and co-workers[46] justified the cellular localization of BODIPY dyes in the various lipid membranes with the lipophilic nature of these compounds, a justification that can also be extended to ADPM derivatives.

To sum up, these preliminary results indicate that the efficiency of these ADPM can be improved by tuning their strong hydrophobicity. Therefore, the encapsulation of these compounds in targeted delivery vehicles may be a suitable strategy to enhance the performance of these photosensitizers.[47-50]

Conclusions

To the best of our knowledge, this work provides the first study on the application of ADPMs as potential photosensitizing agents for PDT. These compounds exhibit some interesting features, including a broad absorption band typically between 500 and 700 nm (or 800 nm in the case of ADPM **4**), high extinction coefficients, and an excellent photostability and chemical versatility, that substantiate the bet on their use as photosensitizers. Taken together, our results clearly demonstrate the potential of these compounds to be used as photosensitizers against B16F10 melanoma cell line, especially the ADPM **2**, bearing two methoxy groups, which demonstrated photocytotoxicity and no-cytotoxicity towards the melanoma cell line B16F10, at a concentration of 2.5 μM. In summary, we conclude that the presence, the number and the strength of the electron-donor groups influence their cytotoxicity. In addition, we also observed that the photodynamic efficiency of these ADPMs is strongly dependent of their tendency to aggregate. These preliminary results could be the starting point for the valorisation of these compounds by themselves, so that they are not only seen as simple precursors for the synthesis of aza-BODIPY dyes. Their encapsulation in nanocarriers, such as polymers, micelles or nanoparticles, can be and efficient strategy to diminish their aggregation tendency and improve PDT efficiency.

Conflicts of interest

The authors declare no conflict of interest.

Acknowledgements

Thanks are due to Fundação para a Ciência e a Tecnologia (FCT) for the financial support to project PTDC/QEQ-QOR/6160/2014, the QOPNA research project (FCT UID/QUI/00062/2019) and

the LAQV-REQUIMTE (UIDB/50006/2020), the project CICECO–Aveiro Institute of Materials, POCI-01-0145-FEDER-007679 (FCT UID/CTM/50011/2019), through national funds and where applicable co-financed by the FEDER, within the PT2020 Partnership Agreement. Thanks are also due to Conselho Nacional de Desenvolvimento Científico e Tecnológico (CNPq), Coordenação de Aperfeiçoamento de Pessoal de Nível Superior (CAPES), Fundação de Amparo à Pesquisa do Estado de São Paulo (FAPESP- 2016/12707-0), Universidade de São Paulo. L.D. Costa thanks FCT for her doctoral grant (SFRH/PD/BD/114578/2016). S. Guieu acknowledges the funding from national funds (OE), through FCT –, in the scope of the framework contract foreseen in the numbers 4, 5 and 6 of the article 23, of the Decree-Law 57/2016, of August 29, changed by Law 57/2017, of July 19, and from the Integrated Programme of SR&TD "pAGE – Protein aggregation Across the Lifespan" (reference CENTRO-01-0145-FEDER-000003). K.A.D.F. Castro thanks PNPD/CAPES for her postdoctoral grant.

Notes and references

1 M. A. T. Rogers, *Nature*, 1943, **151**, 504-504.
2 M. A. T. Rogers, *J. Chem. Soc.*, 1943, DOI: 10.1039/JR9430000590, 590-596.
3 A. Gorman, J. Killoran, C. O'Shea, T. Kenna, W. M. Gallagher and D. F. O'Shea, *J. Am. Chem. Soc.*, 2004, **126**, 10619-10631.
4 S. O. McDonnell and D. F. O'Shea, *Org. Lett.*, 2006, **8**, 3493-3496.
5 M. Grossi, A. Palma, S. O. McDonnell, M. J. Hall, D. K. Rai, J. Muldoon and D. F. O'Shea, *J. Org. Chem.*, 2012, **77**, 9304-9312.
6 M. J. Hall, S. O. McDonnell, J. Killoran and D. F. O'Shea, *J. Org. Chem.*, 2005, **70**, 5571-5578.
7 A. Bessette, M. Cibian, F. Bélanger, D. Désilets and G. S. Hanan, *Phys. Chem. Chem. Phys.*, 2014, **16**, 22207-22221.
8 A. Gut, Ł. Łapok, D. Jamróz and M. Nowakowska, *Asian J. Org. Chem.*, 2017, **6**, 207-223.
9 K. I. Lugovik, A. K. Eltyshev, P. O. Suntsova, L. T. Smoluk, A. V. Belousova, M. V. Ulitko, A. S. Minin, P. A. Slepukhin, E. Benassi and N. P. Belskaya, *Org. Biomol. Chem.*, 2018, **16**, 5150-5162.
10 S. Callaghan, M. A. Filatov, H. Savoie, R. W. Boyle and M. O. Senge, *Photochem. Photobiol. Sci.*, 2019, **18**, 495-504.
11 B. Brandes, S. Hoenke, L. Fischer and R. Csuk, *Eur. J. Med. Chem.*, 2020, **185**, 111858.
12 Y. Ge and D. F. O'Shea, *Chem. Soc. Rev.*, 2016, **45**, 3846-3864.
13 W. Senevirathna, C. M. Daddario and G. Sauvé, *J. Phys. Chem. Lett.*, 2014, **5**, 935-941.
14 S. Pejić, A. M. Thomsen, F. S. Etheridge, R. Fernando, C. Wang and G. Sauvé, *J. Mater. Chem. C*, 2018, **6**, 3990-3998.
15 I. V. Aksenova, R. T. Kuznetsova, I. P. Pozdnyakov, V. F. Plyusnin, M. B. Berezin, N. A. Bumagina, E. S. Jarnikova, M. V. Parkhats and B. M. Dzhagarov, *J. Photochem. Photobiol. A*, 2017, **344**, 206-211.
16 T. S. Teets, D. V. Partyka, J. B. Updegraff and T. G. Gray, *Inorg. Chem.*, 2008, **47**, 2338-2346.
17 L. Gao, N. Deligonul and T. G. Gray, *Inorg. Chem.*, 2012, **51**, 7682-7688.
18 K. Chanawanno, A. Hasheminasab, J. T. Engle and C. J. Ziegler, *Polyhedron*, 2015, **101**, 276-281.
19 D. V. Partyka, N. Deligonul, M. P. Washington and T. G. Gray, *Organometallics*, 2009, **28**, 5837-5840.
20 T. S. Teets, J. B. Updegraff, A. J. Esswein and T. G. Gray, *Inorg. Chem.*, 2009, **48**, 8134-8144.
21 W. Senevirathna, J.-y. Liao, Z. Mao, J. Gu, M. Porter, C. Wang, R. Fernando and G. Sauvé, *J. Mater. Chem. A*, 2015, **3**, 4203-4214.
22 Q. Tang, W. Xiao, C. Huang, W. Si, J. Shao, W. Huang, P. Chen, Q. Zhang and X. Dong, *Chem. Mater.*, 2017, **29**, 5216-5224.
23 G. R. McKeown, J. G. Manion, A. J. Lough and D. S. Seferos, *Chem. Commun.*, 2018, **54**, 8893-8896.
24 H. Cai, E. A. Cho, Y. Li, J. Sockler, C. R. Parish, B. H. Chong, J. Edwards, T. J. Dodds, P. M. Ferguson, J. S. Wilmott, R. A. Scolyer, G. M. Halliday and L. M. Khachigian, *Oncogene*, 2018, **37**, 5115-5126.
25 D. Coricovac, C. Dehelean, E. A. Moaca, I. Pinzaru, T. Bratu, D. Navolan and O. Boruga, *Int. J. Mol. Sci.*, 2018, **19**.
26 G. Mattia, R. Puglisi, B. Ascione, W. Malorni, A. Care and P. Matarrese, *Cell Death Dis.*, 2018, **9**, 112.
27 I. Baldea, L. Giurgiu, I. D. Teacoe, D. E. Olteanu, F. C. Olteanu, S. Clichici and G. A. Filip, *Curr. Med. Chem.*, 2018, **25**, 5540-5563.
28 B. Domingues, J. M. Lopes, P. Soares and H. Pópulo, *Immunotargets Ther.*, 2018, **7**, 35-49.
29 I. Kozar, C. Margue, S. Rothengatter, C. Haan and S. Kreis, *Biochim. Biophys. Acta*, 2019, **1871**, 313-322.
30 C. Frochot and S. Mordon, *J. Porphyrins Phthalocyanines*, 2019, **23**, 347-357.
31 K. A. D. F. Castro, N. M. M. Moura, F. Figueira, R. I. Ferreira, M. M. Q. Simões, J. A. S. Cavaleiro, M. A. F. Faustino, A. J. D. Silvestre, C. S. R. Freire, J. P. C. Tomé, S. Nakagaki, A. Almeida and M. G. P. M. S. Neves, *Int. J. Mol. Sci.*, 2019, **20**.
32 J. Bhaumik, R. Weissleder and J. R. McCarthy, *J. Org. Chem.*, 2009, **74**, 5894-5901.
33 J. S. Dos Santos, L. C. Ramos, L. P. Ferreira, V. L. Campo, L. C. D. de Rezende, F. da Silva Emery and R. Santana da Silva, *Nitric Oxide*, 2019, **86**, 38-47.
34 A. G. Griesbeck and A. Bartoschek, *Chem. Commun.*, 2002, DOI: 10.1039/B204017D, 1594-1595.
35 F. Cardona, J. Rocha, A. M. S. Silva and S. Guieu, *Dyes Pigments*, 2014, **111**, 16-20.
36 J. Killoran, L. Allen, J. F. Gallagher, W. M. Gallagher and D. F. O'Shea, *Chem. Commun.*, 2002, DOI: 10.1039/B204317C, 1862-1863.
37 X.-D. Jiang, J. Guan, J. Zhao, B. Le Guennic, D. Jacquemin, Z. Zhang, S. Chen and L. Xiao, *Dyes Pigments*, 2017, **136**, 619-626.
38 N. Epelde-Elezcano, V. Martínez-Martínez, E. Peña-Cabrera, C. F. A. Gómez-Durán, I. L. Arbeloa and S. Lacombe, *RSC Adv.*, 2016, **6**, 41991-41998.
39 A. Kamkaew, S. H. Lim, H. B. Lee, L. V. Kiew, L. Y. Chung and K. Burgess, *Chem. Soc. Rev.*, 2013, **42**, 77-88.
40 S. Kwiatkowski, B. Knap, D. Przystupski, J. Saczko, E. Kędzierska, K. Knap-Czop, J. Kotlińska, O. Michel, K. Kotowski and J. Kulbacka, *Biomed. Pharmacother.*, 2018, **106**, 1098-1107.
41 40 E. J. Hong, D. G. Choi and M. S. Shim, *Acta Pharm . Sin. B*, 2016, **6**, 297-307.
42 X. Yi, J. Dai, Y. Han, M. Xu, X. Zhang, S. Zhen, Z. Zhao, X. Lou and F. Xia, *Commun . Biol.*, 2018, **1**, 202.
43 T. Gayathri, A. K. Barui, S. Prashanthi, C. R. Patra and S. P. Singh, *RSC Adv.*, 2014, **4**, 47409-47413.
44 C. S. Oliveira, R. Turchiello, A. J. Kowaltowski, G. L. Indig and M. S. Baptista, *Free Radic. Biol. Med.*, 2011, **51**, 824-833.
45 R. D. Moriarty, A. Martin, K. Adamson, E. O'Reilly, P. Mollard, R. J. Forster and T. E. Keyes, *J. Microsc.*, 2014, **253**, 204-218.
46 R. Lincoln, A. M. Durantini, L. E. Greene, S. R. Martinez, R. Knox, M. C. Becerra and G. Cosa, *Photochem. Photobiol. Sci.*, 2017, **16**, 178-184.
47 T. Gayathri, A. Vijayalakshmi, S. Mangalath, J. Joseph, N. M. Rao and S. P. Singh, *ACS Med. Chem. Lett.*, 2018, **9**, 323-327.

View Article Online
DOI: 10.1039/D0PP00114G

48 K. Chansaenpak, S. Tanjindaprateep, N. Chaicharoenaudomrung, O. Weeranantanapan, P. Noisa and A. Kamkaew, *RSC Adv.*, 2018, **8**, 39248-39255.
49 W. Hu, H. Ma, B. Hou, H. Zhao, Y. Ji, R. Jiang, X. Hu, X. Lu, L. Zhang, Y. Tang, Q. Fan and W. Huang, *ACS Appl. Mater. Interfaces*, 2016, **8**, 12039-12047.
50 M. Sadasivam, P. Avci, G. K. Gupta, S. Lakshmanan, R. Chandran, Y. Y. Huang, R. Kumar and M. R. Hamblin, *Eur. J. Nanomed.*, 2013, **5**, 115-129.

View Article Online
DOI: 10.1039/D0PP00114G

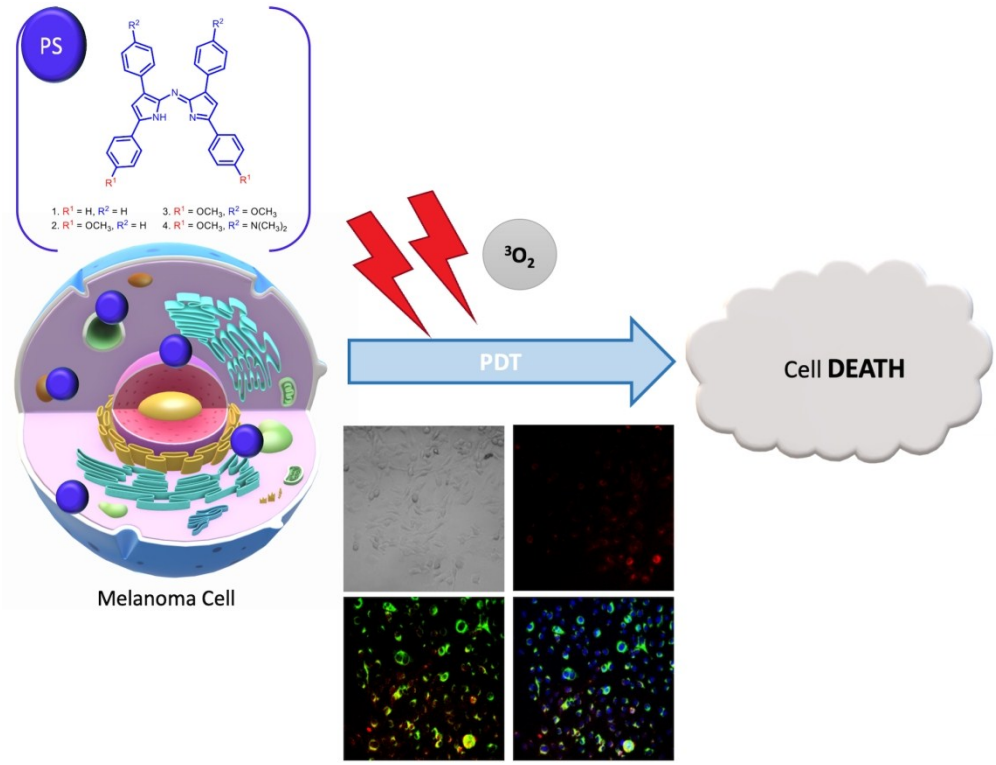

81x61mm (600 x 600 DPI)